

SCIENTIFIC REPORTS



OPEN

Enhanced anastomotic healing by Daikenchuto (TJ-100) in rats

Toshiaki Wada¹, Kenji Kawada¹, Kenjiro Hirai^{1,2}, Kosuke Toda¹, Masayoshi Iwamoto³, Suguru Hasegawa⁴ & Yoshiharu Sakai¹

Received: 25 September 2017

Accepted: 3 January 2018

Published online: 18 January 2018

Daikenchuto (DKT), a traditional Japanese medicine, is widely used to treat various gastrointestinal disorders. This study aimed to investigate whether DKT could promote the anastomotic healing in a rat model. Pedicled colonic segments were made in left colon by ligation of the feeding arteries, and then intestinal continuity was restored. Colonic blood flow was analyzed by using ICG fluorescence imaging: Fmax, Tmax, T1/2, and Slope were calculated. Anastomotic leakage (AL) was found in 6 of 19 rats (31.6%) in the control group, whereas in 1 of 16 rats (6.2%) in the DKT group. The Fmax and Slope of DKT group were significantly higher than those of control group. DKT could promote the anastomotic healing, with the higher bursting pressure on postoperative day (POD) 2 and 5, the larger granulation thickness on POD 5, and neoangiogenesis on POD 5. Histological examination showed DKT exhibited a decreased inflammatory cell infiltration, enhanced fibroblast infiltration, and enhanced collagen density on POD 5. In the DKT group, the levels of TGFβ1 on POD 2 and VEGFα on POD5 were significantly higher, whereas the level of TNFα on POD 2 was significantly lower. Therefore, DKT could be effective for the prevention of AL following colorectal surgery.

Anastomotic leakage (AL) is the most dreaded complication after colorectal surgery and is known to cause high morbidity and mortality. The reported rate of AL following colorectal surgery remains approximately 10% worldwide^{1,2}. The pathophysiology of AL remains unclear, although numerous studies have been conducted on animals and humans. Despite the multifactorial etiology of AL, vascular perfusion is considered critical to anastomotic healing. Therefore, objective and accurate measurements of the intestinal perfusion are necessary to reduce the AL rate. Although several methods, including doppler technology and oxygen spectroscopy, have been proposed to assess intestinal perfusion, they are still experimental and cannot be used in regular clinical applications. In recent years, near-infrared (NIR) fluorescence technology with indocyanine green (ICG) has emerged as the most promising method to enable an accurate evaluation of the intestinal perfusion^{3–5}. ICG is a cyanine dye and its fluorescence imaging is based on the principal that plasma protein-bound ICG emits light with a wavelength of 830 nm when illuminated by NIR light of 760–780 nm. Therefore, it can reveal the presence of an ischemic perfusion before performing the anastomosis.

Daikenchuto (DKT) is a traditional Japanese medicine (Kampo) that is a mixture of extract powders from dried Japanese pepper, processed ginger, ginseng radix, and maltose powder. DKT is reported to have three major effects: (i) improvement of intestinal movement, (ii) up-regulation of colonic blood flow, and (iii) activation of anti-inflammatory effect^{6–9}. The anti-inflammatory effect is attributable to the down-regulation of cyclooxygenase-2 and the up-regulation of endogenous adrenomedullin^{6,7}. An increase in intestinal blood flow is due to the up-regulation of calcitonin gene-related peptide⁸. Accelerated intestinal motility is due to modulation of intestinal contraction and relaxation by the release of acetylcholine, nitric oxide, and other excitatory neurotransmitters¹⁰. DKT is widely used for the treatment of various gastrointestinal disorders, including postoperative ileus and ischemic intestinal disorders¹¹. Moreover, a randomized, double-blind study on healthy humans in the United States indicated that DKT significantly accelerated intestinal transit in the small intestine and ascending colon¹². Several randomized controlled trials on the patients with postoperative ileus, Crohn's disease, functional constipation and irritable bowel syndrome are currently on-going in the United States and Japan.

¹Department of Surgery, Graduate School of Medicine, Kyoto University, Kyoto, Japan. ²Department of Surgery, Otsu City Hospital, Otsu, Shiga, Japan. ³Department of Surgery, National Hospital Organization Himeji Medical Center, Himeji, Japan. ⁴Department of Gastroenterological Surgery, Faculty of Medicine, Fukuoka University, Fukuoka, Japan. Correspondence and requests for materials should be addressed to K.K. (email: kkawada@kuhp.kyoto-u.ac.jp)

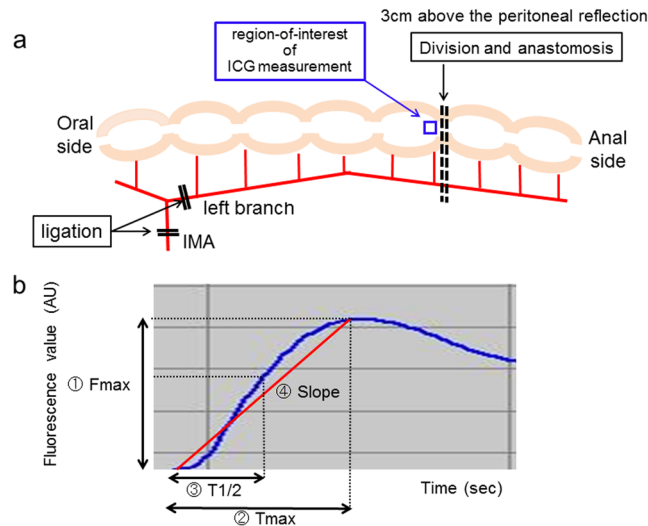


Figure 1. (a) A schematic representation of the model used in this study. Inferior mesenteric artery (IMA) and its left branch were sequentially ligated, and then the distal colon was transected 3 cm above the peritoneal reflection. ICG fluorescence measurement was performed at the distal end of the pedicled segment (blue square point). After ICG fluorescence measurement, intestinal continuity was restored by an end-to-end anastomosis. (b) Time curve of ICG fluorescence intensity. Fmax (the magnitude of intensity from the onset of ICG to the maximum intensity), Tmax (time from the onset of ICG to the maximum intensity), T1/2 (time required to reach the half of maximum from the onset of ICG), and Slope (Fmax/Tmax).

We hypothesized that DKT may prevent AL via its above-mentioned effects. Therefore, the aim of this study was to investigate whether DKT could promote the anastomotic healing following colorectal surgery in an AL rat model.

Materials and Methods

Animals. Wistar rats (8 weeks; Japan SLC, Shizuoka, Japan) were used for the animal experiments. DKT was provided from Tsumura & Co (Tokyo, Japan). All animal experiments were performed in accordance with the International Guiding Principles for Biomedical Research Involving Animals, and this study protocol was approved by the Animal Care and Use Committee of Kyoto University.

Experimental Protocol. Thirty five rats were divided into the two groups: the control group (n = 19) and the DKT group (n = 16). The rats were sacrificed on postoperative day (POD) 2 or POD 5. In the DKT group, DKT (300 mg/kg) was administered orally 1 hour before the operation and one time per day from POD 1 to POD 2 (n = 8) or POD 5 (n = 8). In the control group, distilled water was administered 1 hour before the operation and one time per day from POD 1 to POD 2 (n = 10) or POD 5 (n = 9).

Surgical Procedures. After a 3-cm midline laparotomy was performed, the pedicle segment of the colon was created by sequentially ligating the inferior mesenteric artery (IMA) and its left branch (Fig. 1a), which was modified from the ischemia colon model previously reported by Posma *et al.*¹³. Before bowel resection, the NIR camera system (PDE-neo system; Hamamatsu Photonics K.K., Hamamatsu, Japan) was fixed 15 cm away from the pedicled ischemic colon for the analysis of colonic blood flow, taking the focal distance of this system into consideration (Supplementary Fig. 1a). The distal colon was transected 3 cm above the peritoneal reflection. After ICG fluorescence imaging movie was recorded, intestinal continuity was restored by an end-to-end anastomosis (8 stitches of interrupted sutures using 6-0 PDS). The anastomotic site was evaluated on POD 2 (n = 18) or POD 5 (n = 17). At sacrifice on POD 2 or POD 5, the anastomotic site was graded from 1 to 3, as previously described¹⁴; (1) no, AL (2) small abscess at the anastomotic site < 1 cm³, (3) large (> 1 cm³) abscess at the anastomotic site, or (4) complete dehiscence with peritonitis/death due to faecal peritonitis. Grades 2, 3 and 4 were defined as AL. All surgical procedures were performed by a board-certified surgeon (T.W.).

Measurement of Colonic Blood Flow. During the operation, the colonic blood flow was analyzed using ICG fluorescence imaging. We used a PDE-neo system and a luminance analysis software (ROIs; Hamamatsu Photonics K.K.) for the quantitative evaluation of ICG fluorescence (Supplementary Fig. 1). The stored video files were analyzed retrospectively by using the software, ROIs¹⁵⁻¹⁷. In the quantitative measurement, the region-of-interest was positioned at the transection site (Fig. 1a). A time-dependent curve of fluorescence intensity was constructed, and the following 4 parameters were calculated: Fmax (the magnitude of intensity from the onset of ICG to the maximum intensity), Tmax (time from the onset of ICG to the maximum intensity), T1/2 (time required to reach the half of maximum from the onset of ICG), and Slope (Fmax/Tmax) (Fig. 1b).

Measurement of Bursting Pressure. On POD 2 or POD 5, a 5-cm segment of colon including the anastomotic site with adherent organs was resected en bloc. A diameter 3 mm catheter was placed into the oral side of the descending colon, and both sides of the colon were ligated to close the lumen. The catheter was connected to an infusion syringe and a manometer (Handy Manometer PG-100B; Copal Electronics, Tokyo, Japan). The bursting pressure of the anastomosis was measured as the intraluminal pressure at which air leakage from the anastomosis was initially observed.

Histopathological Assessment. After measuring the bursting pressure, samples containing the anastomotic site were fixed in a 4 wt% formaldehyde solution and embedded in paraffin. Sections (5 μ m) were cut and stained with hematoxylin and eosin (H&E). For the histological grading scale, infiltration of inflammatory cells (i.e., lymphocytes, plasma cells, and polymorphonuclear leucocytes) or fibroblasts were evaluated at the anastomotic site using a modified 0-to-4 Ehrlich and Hunt numerical scale: 0 = no evidence, 1 = occasional evidence, 2 = light scattering, 3 = abundant evidence and 4 = confluent cells or fibers¹⁸. The sections were viewed systemically at $\times 100$ magnification. Regarding collagen density, collagen deposition at the anastomotic site was scored using the same scale. The sections were stained with anti-type III collagen antibody (SouthernBiotech, Birmingham, AL; I330-01) and scanned systemically at $\times 200$ magnification. All assessments were conducted by two researchers (T.W., and K.H.) blinded to the experimental groups.

Thickness of Granulation. The thickness of the granulation tissue at the anastomotic site was measured. The H&E sections were viewed systemically at $\times 40$ magnification. Granulation tissues were morphologically identified as tissues containing collagen fibers, fibroblasts, microvessels and inflammatory cells in the center part of the anastomotic site. The measurement was performed for three sections and the average was calculated.

Neovascularization at the Anastomotic Site. The sections were stained with anti-von Willebrand factor (vWF) (Abcam, Cambridge, UK; ab6994) and scanned systemically at $\times 400$ magnification. The vWF-positive blood vessels were counted at the anastomotic site (3 fields (1 mm²) analyzed per sample). The measurement was performed for three sections and the average was calculated.

Measurement of Inflammatory Cytokines by Quantitative Reverse Transcription Polymerase Chain Reaction (RT-PCR). On POD 2 (n = 7) or POD 5 (n = 8), samples containing the well-healed anastomotic site were resected and stocked in a refrigerator of -80 degrees. Total RNAs were extracted and reverse transcription was carried out. The resulting cDNA was quantified using StepOnePlus™ Real-Time PCR System (Applied Biosystems) and THUNDERBIRD SYBR qPCR Mix (TOYOBO). Primer sequences for GAPDH, IL6, TNF α , IFN γ , TGF β 1, IL10, IL1 β and VEGF α were listed in Supplementary Table 1.

Statistical Analysis. All values were expressed as the means \pm standard deviation (SD). Continuous variables were determined by Student's *t*-test. The Fisher's exact test was used for comparison and analysis of categorical variables. All analyses were two-sided and a *P* value of <0.05 was considered statistically significant in all analyses. Statistical analyses were conducted with JMP Pro software, 11.0.0 (SAS Institute INC, NC).

Compliance with ethical standards. The experimental protocol was approved by the Animal Care and Use Committee of Kyoto University.

Results

Anastomotic Leakage (AL). In total, AL was found in 6 of 19 rats (31.6%) in the control group at sacrifice, whereas it was in 1 of 16 rats (6.2%) in the DKT group (*P* = 0.09). In the control group, AL was occurred in 4 and 2 rats on POD 2 and POD 5, respectively. In the DKT group, AL was found in 1 rat on POD 2.

Colonic Blood Flow measured by ICG Fluorescence Imaging. To measure the colonic blood flow, intraoperative ICG fluorescence imaging was obtained in all cases. After ligation of the IMA and its left branch, the colonic blood flow of the pedicle segment was analyzed by using ICG fluorescence imaging. The fluorescence intensity of the pedicle segment was gradually decreasing to the anal side, but the demarcation line determined by ICG fluorescence was not found in this model (Supplementary Fig. 1b). With the recorded video images, we retrospectively created a time-fluorescence intensity curve at the point of bowel transection (i.e., 3 cm above the peritoneal reflection) using a software, ROIs: Fmax, Tmax, T1/2, and Slope were measured (Fig. 2 and Supplementary Fig. 2). Regarding the Fmax and Slope, there was a significant difference between the control group and DKT group. The Fmax of the DKT group was significantly higher than that of the control group (70.6 ± 4.5 vs. 42.7 ± 4.2 arbitrary units (AU); *P* < 0.001). The Slope of the DKT group was significantly higher than that of the control group (0.5 ± 0.05 vs. 0.3 ± 0.05 AU/sec; *P* = 0.009). Meanwhile, there was no significant difference between the two groups regarding the T1/2 or Tmax.

Anastomotic Bursting Pressure. The anastomotic bursting pressure significantly increased from POD 2 to POD 5 (Fig. 3). On POD 2, the bursting pressure of the DKT group was significantly higher than that of the control group (31.8 ± 5.8 vs. 13.7 ± 5.4 mmHg; *P* = 0.04). Similarly, on POD 5, the bursting pressure of the DKT group was also significantly higher than that of the control group (143.8 ± 15.7 vs. 80.7 ± 15.7 mmHg; *P* = 0.008).

Furthermore, we examined whether there was a correlation between colonic blood flow and bursting pressure. Fmax and Slope were significantly correlated with the bursting pressure on POD 2 (*P* = 0.009 and 0.004, respectively; Fig. 4a). In addition, Fmax was also significantly correlated with the bursting pressure on POD 5 (*P* = 0.04; Fig. 4b). Meanwhile, T1/2 and Tmax were not correlated with the bursting pressure.

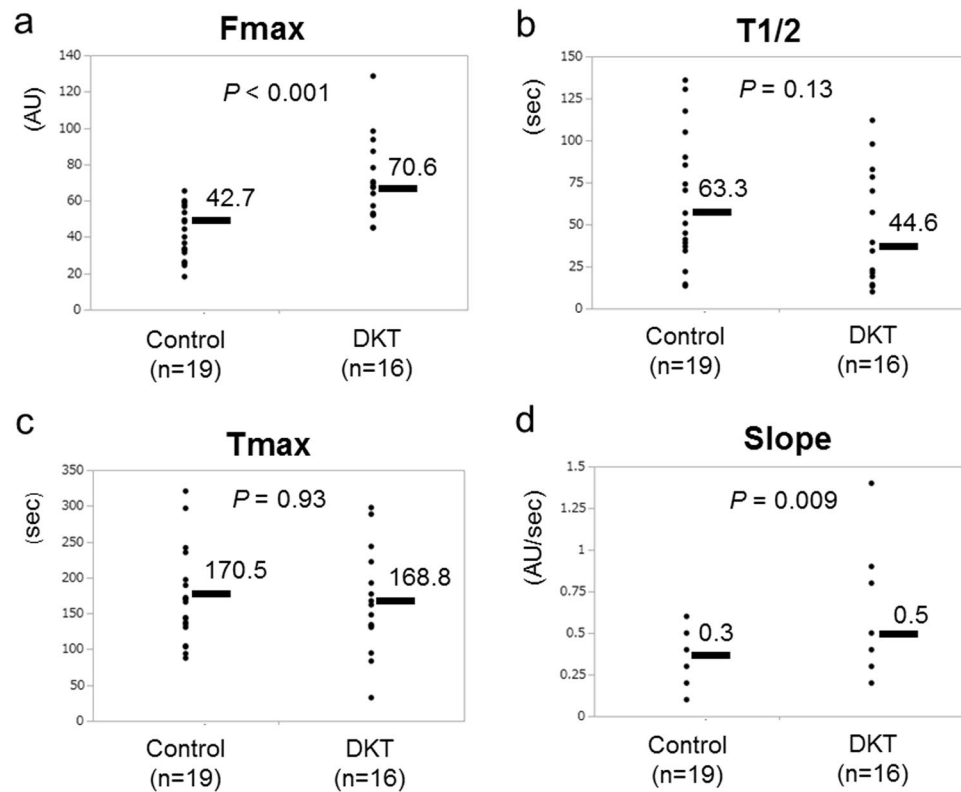


Figure 2. Comparison of ICG fluorescence-related parameters between the control group and DKT group. Fmax (a), T1/2 (b), Tmax (c) and Slope (d). Means bars. Student's t test.

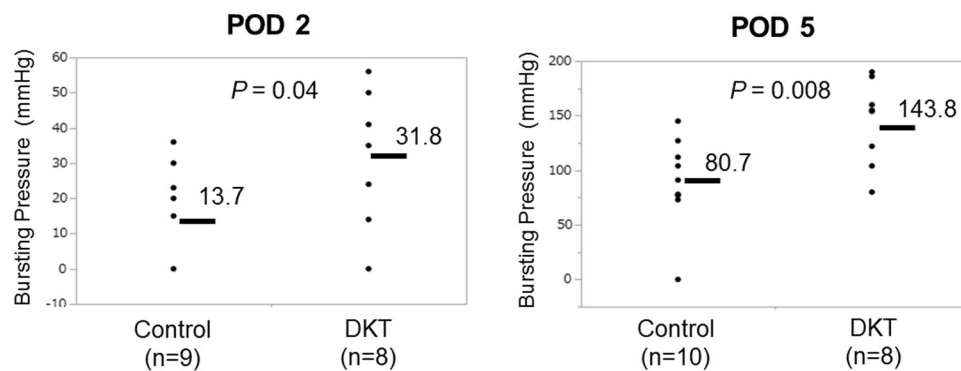


Figure 3. The bursting pressure (mmHg) was measured on POD 2 (left) and 5 (right). Values are expressed as means bar.

We also examined whether there was a correlation between colonic blood flow and AL (Fig. 5). Fmax and Slope of the non-leakage group ($n=7$) were significantly higher than those of the leakage group ($n=28$) ($P=0.01$ and 0.01 , respectively). Meanwhile, Tmax and T1/2 were not significantly correlated with AL.

Histopathological Evaluation. Figure 6 shows the thickness of the granulation tissue. A significant increase in granulation thickness at the anastomotic site was identified on POD 5 for the DKT group compared with the control group (1750 ± 108.2 vs. $989.1 \pm 96.7 \mu\text{m}$; $P < 0.01$). However, no significant difference was found on POD 2 between the two groups (544.2 ± 87.8 vs. $616 \pm 82.8 \mu\text{m}$; $P=0.55$).

The levels of inflammatory cell infiltration, fibroblast infiltration, and collagen density at the anastomotic site were evaluated according to the modified Ehrlich and Hunt numerical scale¹⁸ (Supplementary Table 2 and Supplementary Fig. 3). Inflammatory cell infiltration was marked on POD 2, while fibroblast infiltration and collagen density were marked on POD 5. On POD 2, there were no significant differences between the DKT group and the control group. Meanwhile, on POD 5, the DKT group exhibited decreased inflammatory cell infiltration, enhanced fibroblast infiltration, and enhanced collagen density, although the differences were not statistically significant ($P=0.12$, 0.06 , and 0.15 , respectively).

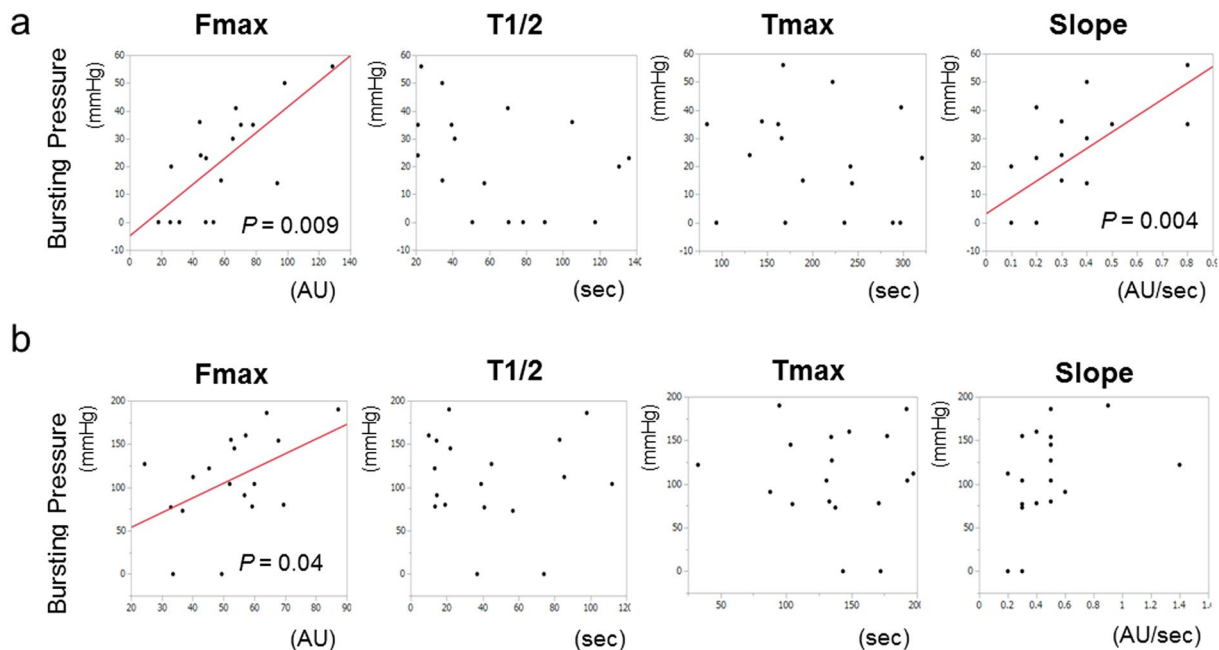


Figure 4. Relationship between the bursting pressure and ICG fluorescence-related 4 parameters. POD 2 (a) and POD 5 (b).

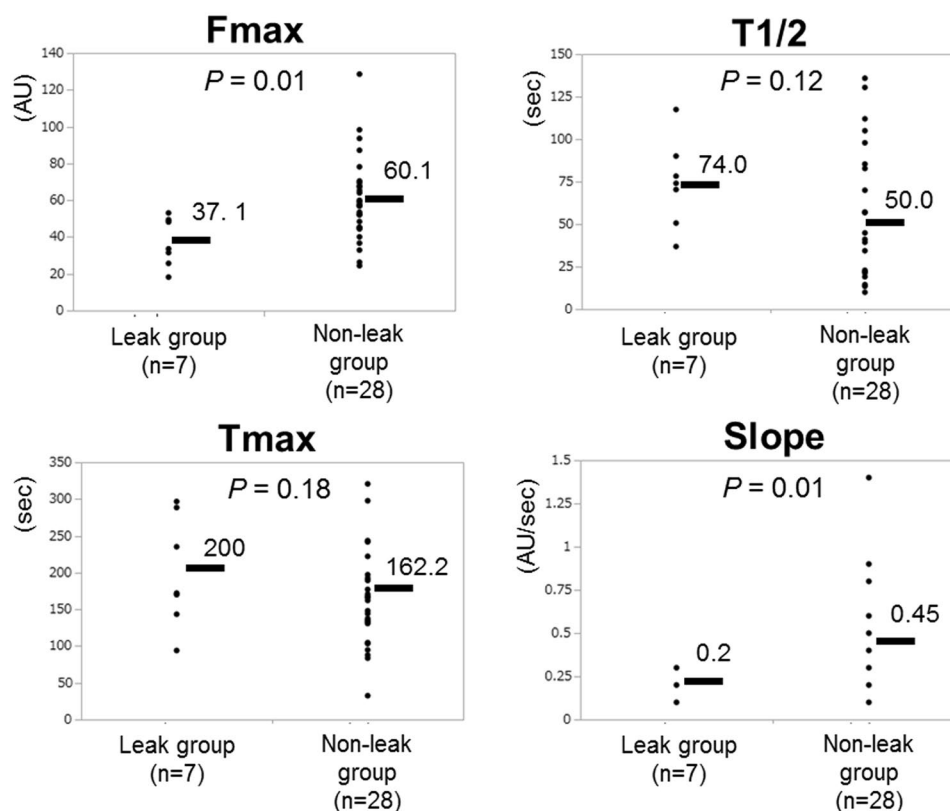


Figure 5. Comparison of ICG fluorescence-related 4 parameters between the leak group (n = 7) and non-leak group (n = 28).

Figure 7 shows the number of vWF-positive blood vessels at the anastomotic site (3 fields (1 mm²)). On POD 2, there were no significant differences between the two groups. Meanwhile, on POD 5, the number of vWF-positive blood vessels in the DKT group was significantly higher than that in the control group (4.2 ± 0.28 vs. 2.7 ± 0.25 vessels/mm²; P = 0.001)

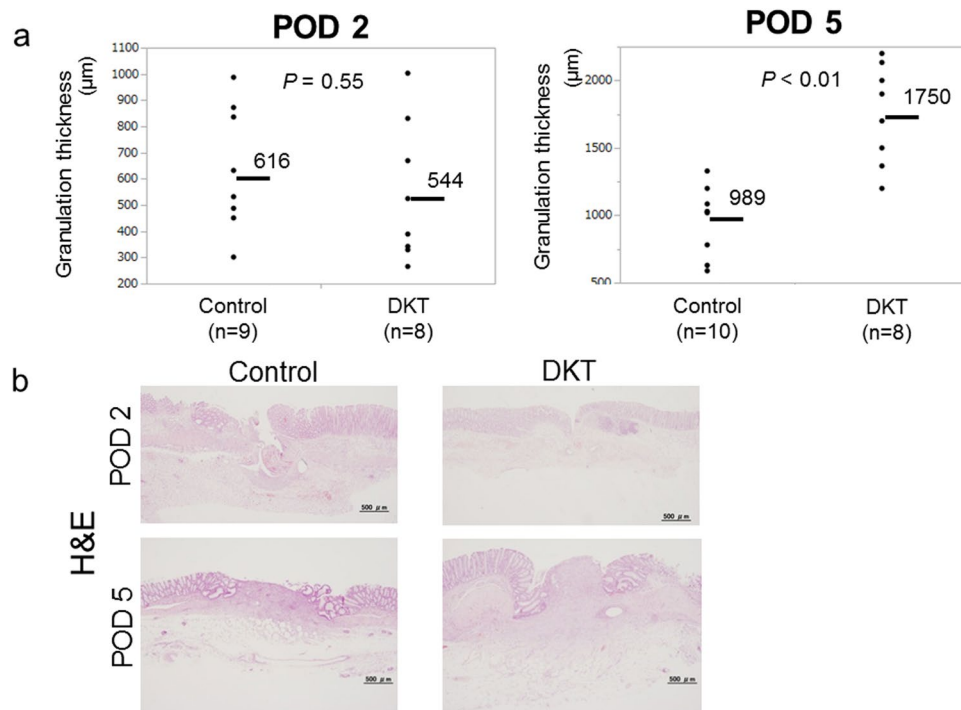


Figure 6. (a) Comparison of granulation thickness between the control group and DKT group on POD 2 (left) and 5 (right). Means bars. Student's t test. (b) Histological sections of the anastomosed site on POD 2 (upper) and 5 (lower) with hematoxylin and eosin (H&E). $\times 40$.

Inflammatory Cytokines at the Anastomotic Site. Figure 8 shows the mRNA expression levels of inflammatory cytokines (TNF α , IL6, IL1 β , TGF β 1, IL10, IFN γ , and VEGF α) measured by quantitative RT-PCR at the well-healed anastomotic site. In the DKT group, on POD 2, TGF β 1 was significantly increased ($P=0.03$), while TNF α was significantly decreased ($P=0.04$). On POD 5, only VEGF α was significantly increased in the DKT group ($P=0.01$). Meanwhile, there was no significant difference between the two groups as to the other cytokines.

Discussion

DKT has been clinically used to treat various gastrointestinal diseases, including postoperative ileus, abdominal bloating and cold sensation in the abdomen. DKT has specific functions such as improving intestinal movement, increasing colonic blood flow, and suppressing inflammation. Kono *et al.* reported that DKT could increase intestinal perfusion in rats by up-regulating calcitonin gene-related peptide (CGRP) and adrenomedullin (ADM)^{8,19}. Therefore, we examined whether these effects of DKT could result in the promotion of anastomotic healing following colorectal surgery in an AL rat model. In the present study, Fmax and Slope were significantly higher in the DKT group than in the control group (Fig. 2). Importantly, DKT significantly improved the bursting pressure on both POD 2 and 5 (Fig. 3), the granulation thickness at the anastomotic site on POD 5 (Fig. 6), neoangiogenesis at the anastomotic site on POD 5 (Fig. 7), and the histopathological inflammation scores on POD 5 (Supplementary Table 2). In addition, we examined the effect of DKT on several inflammatory cytokines in this model. In the DKT group, the levels of TGF β 1 on POD 2 and VEGF α on POD5 were significantly higher, whereas that of TNF α on POD 2 was significantly lower (Fig. 8). TGF β 1 plays a role in wound healing and scar formation. VEGF α induces angiogenesis and endothelial cell proliferation, which results in the regulation of vasculogenesis. TNF α is involved in systemic inflammation and one of the cytokines that make up the acute phase reaction. Meanwhile, there was no significant difference between the two groups as to IL6, IL1 β , IL10, and IFN γ (Fig. 8). Previous studies have shown that DKT promotes a variety of growth factors and cytokines, such as TNF α , IFN γ , and IL1 β , that can accelerate the healing of organ injury. In a TNBS-induced colitis model, Kono *et al.* reported that DKT significantly decreased the expressions of TNF α and IFN γ in the colonic mucosa²⁰. In a CPT11-induced intestinal injury model, Chikakiyo *et al.* reported that DKT significantly decreased the expressions of IL1 β and IFN γ in the small intestine²¹. In a T cell transfer-induced colitis model, Iwasa *et al.* reported that DKT significantly decreased IL-17 expression, although the expression levels of TNF α and IFN γ did not change²². In a postoperative ileus model, Endo *et al.* reported that DKT significantly decreased TNF- α expression in the small intestine²³. In a bacterial translocation model, Yoshikawa *et al.* reported that DKT prevented bacterial translocation by maintaining intestinal barrier integrity via anti-apoptotic and anti-inflammatory effects through the reduced expressions of inflammatory cytokines, including IFN γ and TNF α ²⁴.

Recent evidence suggests a role of intestinal bacteria in the pathophysiology of AL. In an AL rat model, *Enterococcus faecalis* contributes to the pathogenesis of AL through collagen degradation and matrix metalloproteinase-9 activation, and that the elimination of *Enterococcus faecalis* through direct topical antibiotics

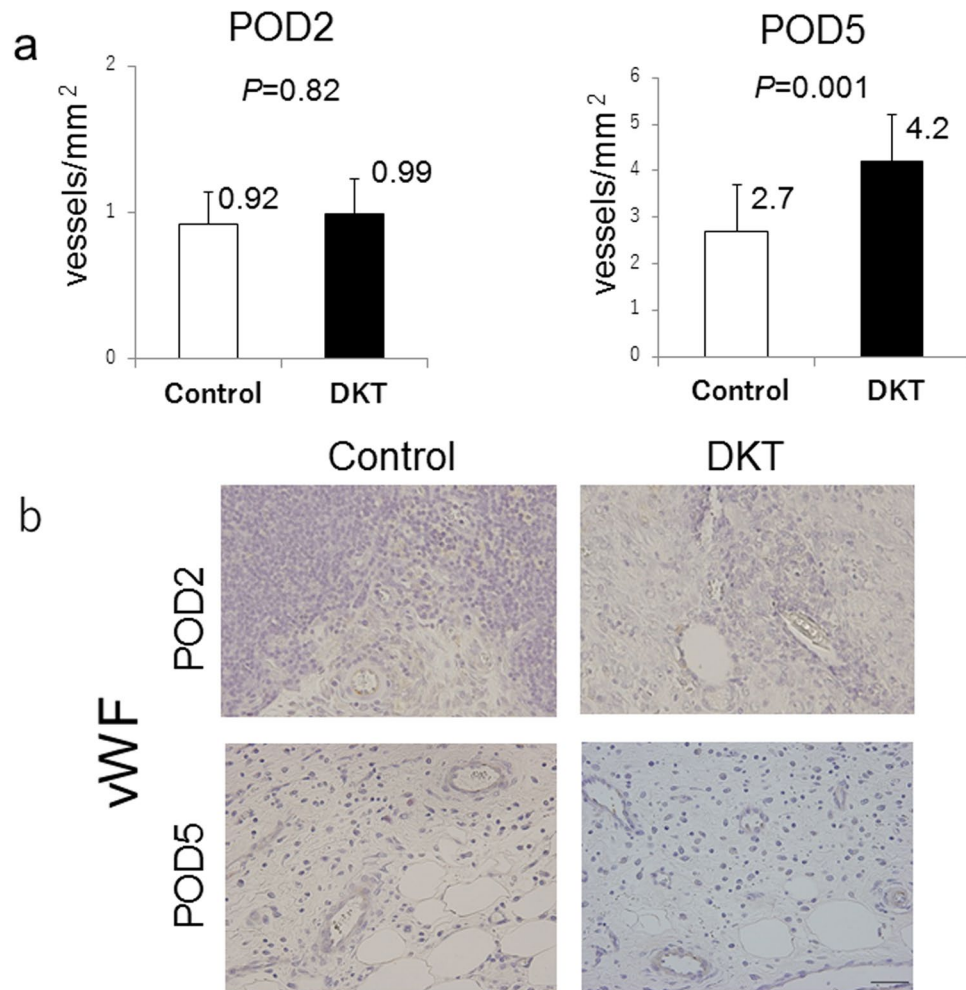


Figure 7. (a) Comparison of neovascularization at the anastomotic site between the control group and DKT group on POD 2 (left) and 5 (right). Means bars. Student's t test. (b) Histological sections of the anastomosed site on POD 2 (upper) and 5 (lower), stained with vWF. $\times 400$.

could prevent AL²⁵. In a rat model of low anterior resection, the combination of preoperative RT and intestinal inoculation with *Pseudomonas aeruginosa* resulted in a higher AL rate²⁶. In addition, it was reported that butyrate, a short-chain fatty acid, produced by microbiota strengthened colonic anastomosis in a rat model²⁷. Notably, Yoshikawa *et al.* reported that DKT prevented the reduction of microbial diversity in the inflammatory intestine of rat, which indicates the new anti-inflammatory effect of DKT through gut microbiome²⁸. However, clinical implications for these findings are lacking. A large retrospective cohort has recently reported that combined preoperative mechanical bowel preparation with oral antibiotics significantly reduces AL and surgical site infection following colorectal surgery²⁹. It remains to be elucidated whether eliminating intestinal bacteria by antibiotics or promoting the growth of certain species by probiotics could improve anastomotic healing.

ICG fluorescence imaging has been used to evaluate blood flow perfusion in several surgical fields such as reconstructive surgery, cardiovascular surgery, and gastrointestinal surgery^{30–32}. Although an NIR camera system can reveal ICG images of blood flow in real time, whether ICG fluorescence imaging is available for preventing AL in the colorectal surgery remains controversial^{4,5,33,34}. In the present study, we investigated colonic blood flow by using ICG fluorescence imaging in an AL animal model. By using luminance analysis software, we quantified the colonic blood flow as four parameters: Fmax, T1/2, Tmax, and Slope. This is the first report to investigate the colonic blood flow by comparing these four parameters in an AL animal model. We found that Fmax and Slope of the colonic blood flow were significantly increased by DKT administration, although T1/2 and Tmax were not (Fig. 2). Posma *et al.* reported that ligation of one feeding artery or three arteries in the colon of rats could reduce the mean Slope to 59% or 26%, respectively, and that there was no significant correlation between Slope and the bursting pressure on POD 2 and 5¹³. Meanwhile, in the present study, Fmax and Slope were significantly correlated with the bursting pressure on POD 2 (Fig. 4a). In addition, Fmax was also significantly correlated with the bursting pressure on POD 5. The differences in animal model, NIR system, and manometer used to measure bursting pressure might account for the differences between the present study and Posma's previous study. In an ischemic bowel animal model, Diana *et al.* reported that lactate level of the 25% Slope area was significantly higher than that of the 75% Slope area, and that the histopathological inflammation score was higher in the 25%

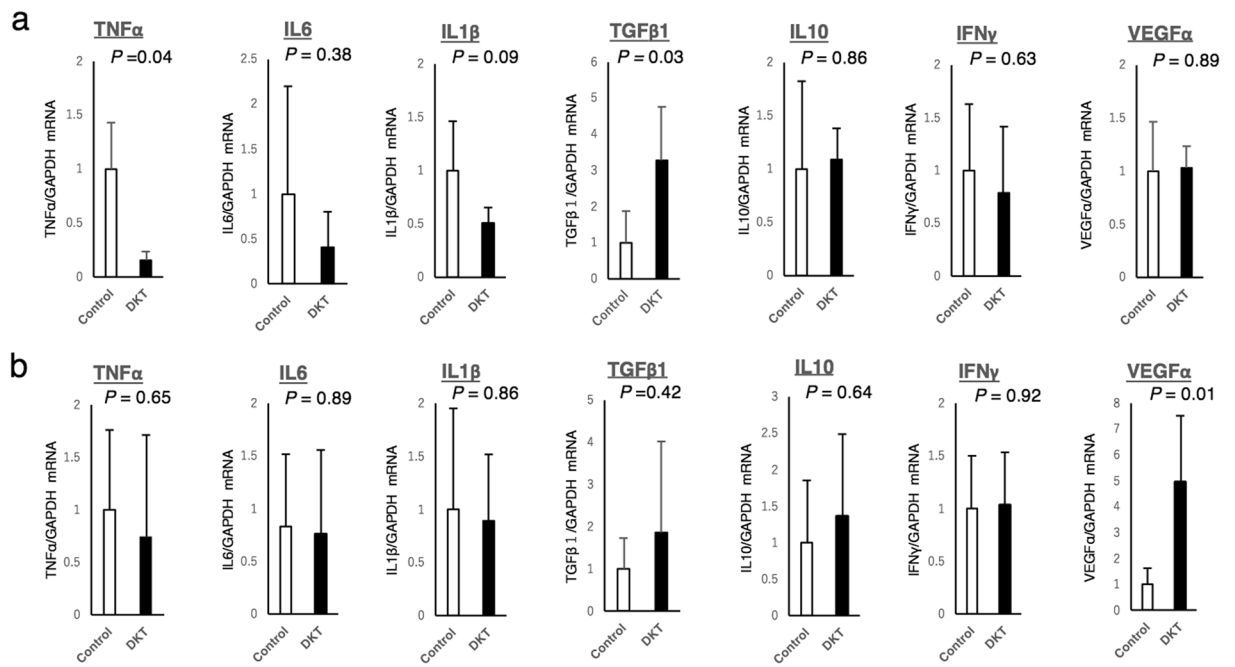


Figure 8. Expression levels of inflammatory cytokines (TNF α , IL6, IL1 β , TGF β 1, IL10, IFN γ and VEGF α) measured by quantitative RT-PCR. POD 2 (a) and POD 5 (b).

Slope area than in the 75% Slope area³⁵. In a porcine model, Nerup *et al.* reported that the regional blood perfusion of the stomach was significantly associated with both Slope and Fmax³⁶. In a small bowel strangulation model, Matsui *et al.* reported that qualitative and/or quantitative metrics, including Fmax, could be predictive of histological grade and animal survival³⁷. In the present study, Fmax and Slope were significantly associated with AL (Fig. 5), which indicates that Fmax and Slope could be predictive of AL. In a clinical setting, we previously reported that preoperative chemotherapy and anticoagulation therapy were significantly correlated to poor intestinal perfusion when evaluated by ICG fluorescence imaging³⁸. In addition, we have recently reported that Fmax and Slope could be predictive of AL from a retrospective analysis of 112 patients who underwent laparoscopic surgery for left-sided colorectal cancers¹⁷, which is consistent with the results of the present animal study.

The present study has some limitations. A systematic review has recently reported that the animal research to investigate AL needs to be improved before results can be applied into the clinical setting³⁹. In addition to the variety of animal models, a wide range of endpoints are used, although the most frequently used surrogate marker of AL in animal models is the bursting pressure of the anastomotic site. Notably, an international consensus statement was reached on several recommendations for the use of animal models for research on AL in the lower gastrointestinal tract⁴⁰.

In conclusion, this study has provided the first evidence of the potential effectiveness of DKT in the prevention of AL following colorectal surgery. The efficacy of DKT for anastomotic healing may be attributable to its capacity to increase blood flow as well as anti-inflammatory effect.

References

- Kang, C. Y. *et al.* Risk factors for anastomotic leakage after anterior resection for rectal cancer. *JAMA Surg.* **148**, 65–71 (2013).
- Matsubara, N. *et al.* Mortality after common rectal surgery in Japan: a study on low anterior resection from a newly established nationwide large-scale clinical database. *Dis Colon Rectum.* **57**, 1075–1181 (2014).
- Kudszus, S., Roesel, C., Schachtrupp, A. & Hoer, J. J. Intraoperative laser fluorescence angiography in colorectal surgery: a noninvasive analysis to reduce the rate of anastomotic leakage. *Langenbecks Arch Surg.* **395**, 1025–1030 (2010).
- Hellan, M., Spinoglio, G., Pigazzi, A. & Lagares-Garcia, J. A. The influence of fluorescence imaging on the location of bowel transection during robotic left-sided colorectal surgery. *Surg Endosc.* **28**, 1695–1702 (2014).
- Jafari, M. D. *et al.* Perfusion assessment in laparoscopic left-sided/anterior resection (PILLAR II): a multi-institutional study. *J Am Coll Surg.* **220**, 82–92 (2015).
- Hayakawa, T. *et al.* Effects of Dai-kenchu-to on intestinal obstruction following laparotomy. *J Smooth Muscle Res.* **35**, 47–54 (1999).
- Kono, T. *et al.* Daikenchuto (TU-100) ameliorates colon microvascular dysfunction via endogenous adrenomedullin in Crohn's disease rat model. *J Gastroenterol.* **46**, 1187–1196 (2011).
- Kono, T. *et al.* Colonic vascular conductance increased by Daikenchuto via calcitonin gene-related peptide and receptor-activity modifying protein 1. *J Surg Res.* **150**, 78–84 (2008).
- Fukuda, H. *et al.* The herbal medicine, Dai-Kenchu-to, accelerates delayed gastrointestinal transit after the operation in rats. *J Surg Res.* **131**, 290–295 (2006).
- Kito, Y. & Suzuki, H. Effects of Dai-kenchu-to on spontaneous activity in the mouse small intestine. *J Smooth Muscle Res.* **42**, 189–201 (2006).
- Kono, T., Kanematsu, T. & Kitajima, M. Exodus of Kampo, traditional Japanese medicine, from the complementary and alternative medicines: is it time yet? *Surgery.* **146**, 837–840 (2009).

12. Manabe, N. *et al.* Effect of daikenchuto (TU-100) on gastrointestinal and colonic transit in humans. *Am J Physiol Gastrointest Liver Physiol.* **298**, G970–975 (2010).
13. Posma, L. A. *et al.* Reduction of oxygenation and blood flow in pedicled bowel segments in the rat and its consequences for anastomotic healing. *Dis Colon Rectum.* **53**, 93–100 (2010).
14. Bosmans, J. *et al.* Comparison of three different application routes of butyrate to improve colonic anastomotic strength in rats. *Int J Colorectal Dis.* **32**, 305–313 (2017).
15. Terasaki, H. *et al.* A quantitative method for evaluating local perfusion using indocyanine green fluorescence imaging. *Ann Vasc Surg.* **27**, 1154–1161 (2013).
16. Kawaguchi, Y. *et al.* Usefulness of Intraoperative Real-Time Tissue Elastography During Laparoscopic Hepatectomy. *J Am Coll Surg.* **221**, e103–111 (2015).
17. Wada T. *et al.* ICG fluorescence imaging for quantitative evaluation of colonic perfusion in laparoscopic colorectal surgery. *Surg Endosc.* 2017 Mar 9. [Epub ahead of print].
18. Ehrlich, H. P., Trarver, H. & Hunt, T. K. Effects of vitamin A and glucocorticoids upon inflammation and collagen synthesis. *Ann Surg.* **177**, 222–227 (1973).
19. Kono, T. *et al.* Epithelial transient receptor potential ankyrin 1 (TRPA1)-dependent adrenomedullin upregulates blood flow in rat small intestine. *Am J Physiol Gastrointest Liver Physiol.* **304**, 428–436 (2013).
20. Kono, T. *et al.* Anti-colitis and -adhesion effects of daikenchuto via endogenous adrenomedullin enhancement in Crohn's disease mouse model. *J Crohn's Colitis.* **4**, 161–170 (2010).
21. Chikakiyo, M. *et al.* Kampo medicine “Dai-kenchu-to” prevents CPT-11-induced small-intestinal injury in rats. *Surg Today.* **42**, 60–67 (2012).
22. Iwasa, T. *et al.* Feeding administration of Daikenchuto suppresses colitis induced by naive CD4+ T cell transfer into SCID mice. *Dig Dis Sci.* **57**, 2571–2579 (2012).
23. Endo, M. *et al.* Daikenchuto, a traditional Japanese herbal medicine, ameliorates postoperative ileus by anti-inflammatory action through nicotinic acetylcholine receptors. *J Gastroenterol.* **49**, 1026–1039 (2014).
24. Yoshikawa, K. *et al.* Kampo medicine “Dai-kenchu-to” prevents bacterial translocation in rats. *Dig Dis Sci.* **53**, 1824–1831 (2008).
25. Shogan, B. D. *et al.* Collagen degradation and MMP9 activation by *Enterococcus faecalis* contribute to intestinal anastomotic leak. *Sci Transl Med.* **7**, 286ra68 (2015).
26. Olivas, A. D. *et al.* Intestinal tissues induce an SNP mutation in *Pseudomonas aeruginosa* that enhances its virulence: possible role in anastomotic leak. *PLoS One.* **7**, e44326 (2012).
27. Bloemen, J. G. *et al.* Butyrate enemas improve intestinal anastomotic strength in a rat model. *Dis Colon Rectum.* **53**, 1069–1075 (2010).
28. Yoshikawa, K. *et al.* Effect of Kampo medicine “Dai-kenchu-to” on microbiome in the intestine of the rats with fast stress. *J Med Invest.* **60**, 221–227 (2013).
29. Kiran, R. P., Murray, A. C., Chiuzan, C., Estrada, D. & Forde, K. Combined preoperative mechanical bowel preparation with oral antibiotics significantly reduces surgical site infection, anastomotic leak, and ileus after colorectal surgery. *Ann Surg.* **262**, 416–425 (2015).
30. Nachiappan, S. *et al.* Intraoperative assessment of colorectal anastomotic integrity: a systematic review. *Surg Endosc.* **28**, 2513–2530 (2014).
31. Still, J. *et al.* Evaluation of the circulation of reconstructive flaps using laser-induced fluorescence of indocyanine green. *Ann Plast Surg.* **42**, 266–274 (1999).
32. Waseda, K. *et al.* Intraoperative fluorescence imaging system for on-site assessment of off-pump coronary artery bypass graft. *JACC Cardiovasc Imaging.* **2**, 604–612 (2009).
33. Boni, L. *et al.* Indocyanine green-enhanced fluorescence to assess bowel perfusion during laparoscopic colorectal resection. *Surg Endosc.* **30**, 2736–2742 (2016).
34. Kin, C., Vo, H., Welton, L. & Welton, M. Equivocal effect of intraoperative fluorescence angiography on colorectal anastomotic leaks. *Dis Colon Rectum.* **58**, 582–587 (2015).
35. Diana, M. *et al.* Intraoperative fluorescence-based enhanced reality laparoscopic real-time imaging to assess bowel perfusion at the anastomotic site in an experimental model. *Br J Surg.* **102**, e169–176 (2015).
36. Nerup, N. *et al.* Quantification of fluorescence angiography in a porcine model. *Langenbecks Arch Surg.* **402**, 655–662 (2017).
37. Matsui, A., Winer, J. H., Laurence, R. G. & Frangioni, J. V. Predicting the survival of experimental ischaemic small bowel using intraoperative near-infrared fluorescence angiography. *Br J Surg.* **98**, 1725–1734 (2011).
38. Kawada, K. *et al.* Evaluation of intestinal perfusion by ICG fluorescence imaging in laparoscopic colorectal surgery with DST anastomosis. *Surg Endosc.* **31**, 1061–1069 (2017).
39. Yauw, S., Wever, K., Hoesseini, A., Ritskes-Hoitinga, M. & van Goor, H. Systematic review of experimental studies on intestinal anastomosis. *Br J Surg.* **102**, 726–734 (2015).
40. Bosmans, J. *et al.* International consensus statement regarding the use of animal models for research on anastomoses in the lower gastrointestinal tract. *Int J Colorectal Dis.* **31**, 1021–1030 (2016).

Acknowledgements

The authors thank Dr. Tatsuaki Tsuruyama (Department of Pathology, Kyoto University, Graduate School of Medicine) for providing fruitful comments regarding Histopathological assessment. We also thank Mr. Takahiro Shikayama (Hamamatsu Photonics K.K.) for technical assistance for the analysis using ROIs. This work was supported by grants from the Ministry of Education, Culture, Sports, Science and Technology of Japan (to K. Kawada).

Author Contributions

T.W., K.K. and S.H. contributed conception and designation of this experiments. T.W., K.K., K.H., K.T. and M.I. performed experiments. T.W. and K.K. wrote the manuscript. All authors discussed the results and approved the manuscript.

Additional Information

Supplementary information accompanies this paper at <https://doi.org/10.1038/s41598-018-19550-4>.

Competing Interests: The authors declare that they have no competing interests.

Publisher's note: Springer Nature remains neutral with regard to jurisdictional claims in published maps and institutional affiliations.



Open Access This article is licensed under a Creative Commons Attribution 4.0 International License, which permits use, sharing, adaptation, distribution and reproduction in any medium or format, as long as you give appropriate credit to the original author(s) and the source, provide a link to the Creative Commons license, and indicate if changes were made. The images or other third party material in this article are included in the article's Creative Commons license, unless indicated otherwise in a credit line to the material. If material is not included in the article's Creative Commons license and your intended use is not permitted by statutory regulation or exceeds the permitted use, you will need to obtain permission directly from the copyright holder. To view a copy of this license, visit <http://creativecommons.org/licenses/by/4.0/>.

© The Author(s) 2018